18. M. A. Krishtal, The Diffusion Mechanism in Iron Alloys [in Russian], Moscow (1972).
19. L. D. Landau and E. M. Lifshits, Statistical Physics [in Russian], Part I, Moscow (1976).
20. V. A. Petrov, Fiz. Tverd. Tela, **25**, No. 10, 3110-3113 (1983).

ANALYSIS OF FORMING THE STRUCTURE AND PROPERTIES OF A METAL DURING LASER HARDENING

V. V. Sobolev and P. M. Trefilov

UDC 621.373.826.004.14

A mathematical model of forming the structure and the properties of a metal under laser treatment involving flashing is proposed. The model takes account of the processes in a transient two-phase zone. It is shown that the parameters of a dendritic structure and excess components, a dislocation density, porous structure characteristics, ultimate strength yield stress, and relative elongation nonmonotonically depend on the laser treatment parameters and metal plate dimensions. The calculated results are in fair agreement with experimental data.

Hardening of metals and alloys involving laser treatment is an effective technology of obtaining high-quality materials [1-4]. Thermal processes during laser treatment with internal heat release at phase transitions are studied in [2]. The urgent problem is the analysis of these processes with an account of a two-phase state of a metal and forecasting of its structure and properties under hardening conditions. These aspects are the subject matter of the present article which is the continuation of work [5] concerned with investigation of the thermal state of a metal under hardening.

We shall consider thermal hardening of an aluminum alloy plate of thickness b, which is much less than its longitudinal dimensions. Let the plate move in the direction of the axis z at velocity w and the laser radiation source be immovable. The axis x runs across the plate and the origin of the Cartesian system (x, z) is on its surface. The process scheme and formulation of the heat problem of metal hardening are given in [5].

Consideration was given to hardening by heat treatment of the plate made of aluminum alloy AMg6. In the basic calculations, b = 20 mm, w = 25 mm/sec, the zone length of laser radiation action was l_c = 0.5 mm, the specific heat flux produced by the radiation q = $6 \cdot 10^8$ W/m^2, temperatures of a cooling medium on the side of the upper and lower surfaces of the plate $T_{b1} = T_{b2}$ = 20°C, and the coefficients of heat transfer from the above surfaces $\alpha = \beta$ = 100 W/m$^2 \cdot$K. As the temperature of hardening completion, T_m = 546°C was assumed, at which a cross section (a portion) of a liquid phase was S = 0.05.

After determining the thermal state of the metal [5], we have analyzed the formation of its crystalline structure. The investigation of structured zones by the procedure described in [6, 7] shows that in the course of metal hardening pillar crystals are mainly formed. They are characterized by two main parameters, i.e., a thickness ξ of dendritic axes of the first order and a distance η between the secondary branches of dendrites [8, 9]:

$$\xi = b_0 [D (T_L - T_m) v_c^{-1}]^{1/2}, \tag{1}$$

$$\eta = a_1 v_c^{-a}. \tag{2}$$

Here D is the diffusion coefficient of an impurity (magnesium); v_c is the cooling rate; a, a_1, b_0 are the numerical coefficients. In calculations, v_c was determined on an isothermal surface of pouring out where a portion of a liquid phase was S = 0.4; b_0 = 1; a = 380, a_1 = 0.4 [10].

Novosibirsk Division of the Scientific-Production Association "The All-Union Institute for Light Alloys." Translated from Inzhenerno-Fizicheskii Zhurnal, Vol. 63, No. 1, pp. 102-108, July, 1992. Original article submitted August 6, 1991.

 1062-0125/92/6301-0732$12.50

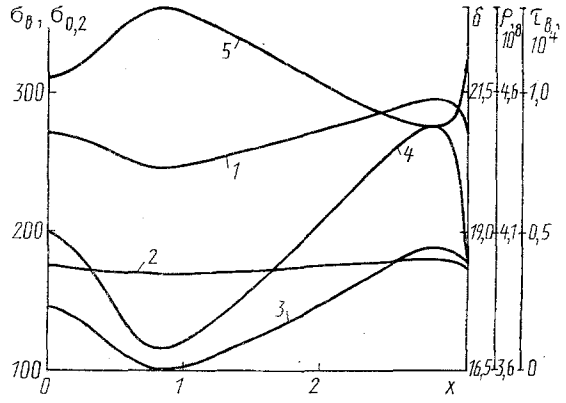

Fig. 1. Distribution of ultimate strength (1), yield stress (2), relative elongation (3), dislocation density (4), and time of complete elimination of intracrystallite liquation (5) with respect to the hardened metal layer. σ_b, $\sigma_{0.2}$, MPa; δ, %; ρ, cm^{-2}; r_b, sec; x, mm.

Also of interest are mean values ξ_a, η_a of the quantities ξ, η, respectively:

$$\xi_a = x_b^{-1} \int_0^{x_b} \xi(x)\, dx, \quad \eta = x_b^{-1} \int_0^{x_b} \eta(x)\, dx. \tag{3}$$

One of the important defects of a metal structure is gas shrinkage porosity. Proceeding from theoretical considerations developed in [11, 12], we may show that the pressure P in the liquid part of a two-phase zone changes as follows:

$$P = P_a + \rho g \zeta_L(z) + \varepsilon \mu w \int_{x_L}^{x} \frac{dx}{mS} \int_{x_L}^{x} \frac{\partial S}{\partial z}\, dx. \tag{4}$$

Here P_a is the atmospheric pressure; g the gravitational acceleration; ε the relative shrinkage; μ the dynamic viscosity; m the permeability of a two-phase zone. As in [11, 12] it is assumed that

$$m(S) = 0{,}125\eta^2 S^3. \tag{5}$$

Within the frames of the quasiequilibrium two-phase zone theory [13] we write:

$$S = [(T_k - T_L)(T_k - T)^{-1}]^{(1-k)^{-1}}. \tag{6}$$

During hardening, the pressure P in a melt decreases due to shrinkage. If it becomes less than P_g of gases in a liquid metal, the melt fails to be continuous, there are formed gas bubbles which because of their small size and large branching of the dendritic structure of a two-phase zone do not evolve from it and after hardening form pores [8, 11]. A failure of the melt continuity occurs at $S = S_*$ and the quantity $V = \varepsilon S_*$ determines the relative volume of pores, while the parameter γ determines their radius [14]:

$$\gamma = 0{,}5\eta \sqrt{V}. \tag{7}$$

The pore density n per unit volume is found from the relation:

$$n = V[V_p(1 - V)]^{-1}, \quad V_p = \frac{4}{3}\pi\gamma^3, \tag{8}$$

where V_p is the volume of a single pore.

The main quantitative structure characteristics of a cast metal include mean thickness m_0, specific surface S_0 and volume fraction Q of excess components, dislocation density ρ_0, ultimate strength σ_b, yield stress $\sigma_{0.2}$, and relative elongation δ. According to [10] the above quantities for the alloy Al–Mg under consideration are expressed in terms of the parameters ξ and η of a dendritic structure as:

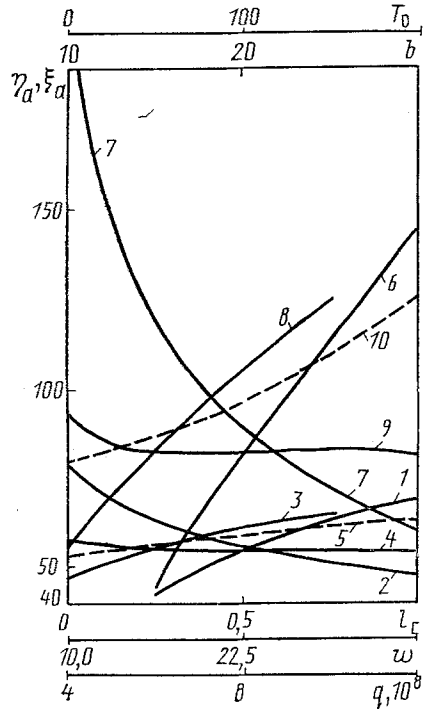

Fig. 2

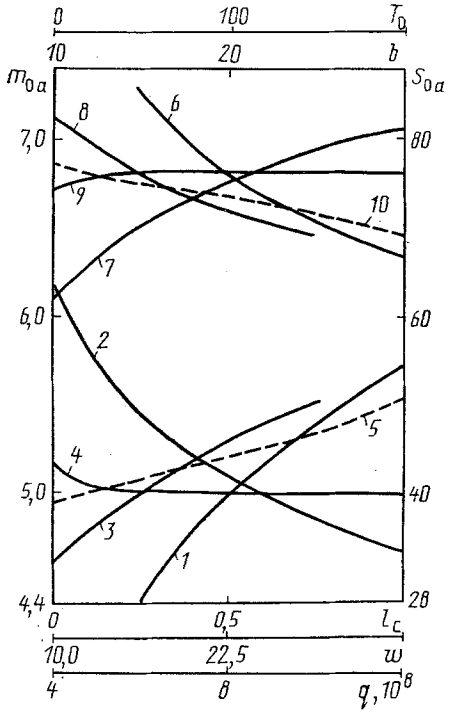

Fig. 3

Fig. 2. Mean values of the dendritic structure parameters η_a (1-5) and ξ_a (6-10) vs l_c (1, 6), w (2, 7), q (3, 8), b (4, 9), and T_0 (5, 10). η_a, ξ_a, μm; l_c, b, mm; w, mm/sec; q, W/m^2; T_0, °C.

Fig. 3. Mean values of the characteristics of inclusions of excess components m_{0a} (1-5) and S_{0a} (6-10) vs l_c (1, 6), w (2, 7), q (3, 8), b (4, 9), and T_0 (5, 10), m_{0a}, μm; S_{0a}, mm^2/mm^3.

$$m_0 = 2{,}3 + 0{,}05\eta, \quad S_0 = 18 \lg v_c, \quad Q = m_0 S_0/40, \quad \rho_0 = 1{,}29 \cdot 10^8 \theta_0 \eta^{-1},$$
$$\sigma_b = 83{,}6 + 52{,}8\xi^{-1/2}, \quad \sigma_{0,2} = 130 + 12{,}4\xi^{-1/2}, \quad \delta = 8{,}36 + 2{,}6\xi^{-1/2}.$$

Here θ_0 is the angle of joining the dendritic cells which, based on experimental data, was taken equal to one degree. In the expression for ρ_0 it is given in radians. The above quantities are measured in the following units: m_0, μm; S_0, mm^2/mm^3, ρ_0, cm^{-2}; Q, δ, %; σ_b, $\sigma_{0.2}$, MPa. The coefficients in the expressions for σ_b, $\sigma_{0.2}$, and δ have been corrected in conformity with the available experimental data [14].

Also of interest in the hardening technology is the time τ_b of complete elimination of intracrystallite liquation at homogenizing annealing of the hardened metal which, in the case of the alloy under discussion, is expressed in terms of η as follows [10]:

$$\tau_b = 1{,}45\eta^2/(\pi^2 D_S),$$

where D_S is the diffusion coefficient of magnesium in a solid phase.

Now let us analyze the calculation results. The parameters of a dendritic structure ξ, η and inclusions of excess components m_0, S_0, Q nonmonotonically change with respect to the height of the hardened layer. The quantities m_0, η, ξ, Q increase in the direction from the upper plane x = 0 to x = b, attain maximum values at x ≈ 0.95 mm, then decrease, become minimal near the lower end of the plate, and increase as far as the plane x = b approaches. The parameter S_0 decreases at a distance from the upper surface of the plate, attains its minimum, then increases, becomes maximal and decreases in the direction of the plane x = b. Such behavior of the above parameters is attributed to the corresponding changes of the temperature gradient G and crystallization rate v_k with respect to the thickness of the hardened metal layer. The quantity G monotonically increases from x = 0 to x = b. The crystallization rate v_k decreases in the same direction. It is at its maximum on the surface x = 0 which also follows from the shape of isotherms abruptly emerging at this surface. As a result, the cooling rate v_c, determined by the

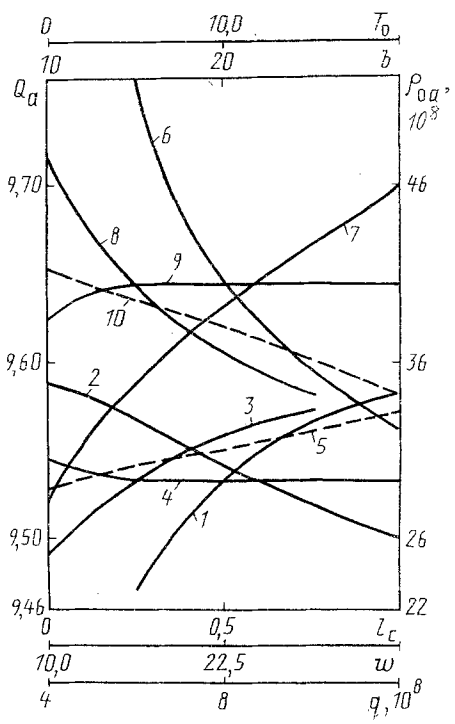

Fig. 4

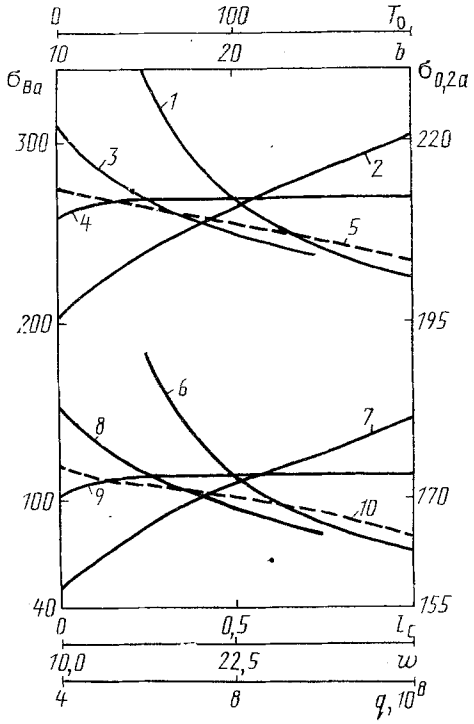

Fig. 5

Fig. 4. Mean values of a volume share of inclusions of excess components Q_a (1-5) and dislocation density ρ_{0a} (6-10) vs l_c (1, 6), w (2, 7), q (3, 8), b (4, 9), and T_0 (5, 10). Q_a, %; ρ_{0a}, cm^{-2}.

Fig. 5. Mean values of ultimate strength σ_{ba} (1-5) and yield stress $\sigma_{0.2a}$ (6, 10) vs l_c (1, 6), w (2, 7), q (3, 8), b (4, 9), and T_0 (5, 10). σ_{ba}, $\sigma_{0.2a}$, MPa.

TABLE 1. Mean Values of the Relative Volume, Radius and Density of Pores Versus the Parameters of Laser Hardening and a Plate

l_c, mm	w, m/s	q, 10^8 W/m^2	b, mm	T_0, °C	V_a, %	γ_a, μm	n_a, 10^{14} м$^{-3}$
0,5	25	6	20	20	0,029	0,53	6,95
0,25	25	6	20	20	0,030	0,48	13,36
1,0	25	6	20	20	0,029	0,45	8,18
0,5	10	6	20	20	0,025	0,42	9,54
0,5	35	6	20	20	0,033	0,51	8,51
0,5	25	4	20	20	0,030	0,51	10,04
0,5	25	10	20	20	0,035	0,50	5,89
0,5	25	6	10	20	0,031	0,36	19,61
0,5	25	6	15	20	0,030	0,44	7,83
0,5	25	6	20	0	0,031	0,69	6,20
0,5	25	6	20	100	0,032	0,51	6,13

product of quantities $v_c = v_k G$ nonmonotonically changes with respect to the thickness of the hardened layer that is responsible for the behavior of η, ξ, m_0, Q, and S_0.

By analogy the mechanical properties of the hardened metal σ_b, δ, $\sigma_{0,2}$, dislocation density ρ_0, and time τ_b nonmonotonically change with respect to the thickness of the hardened layer (Fig. 1). The quantities σ_b, $\sigma_{0.2}$, δ, and ρ_0 decrease at a distance from the upper plate surface, attain their minimum, then increase, attain their maximum near the lower plate end and decrease as they approach it. The parameter τ_b behaves in the same manner as ξ, η.

Mean values of the dendrite parameters ξ_a, η_a increase with l_c, q, T_0 and decreasing of w, b (Fig. 2). After $b \approx 16$, these quantities practically do not change.

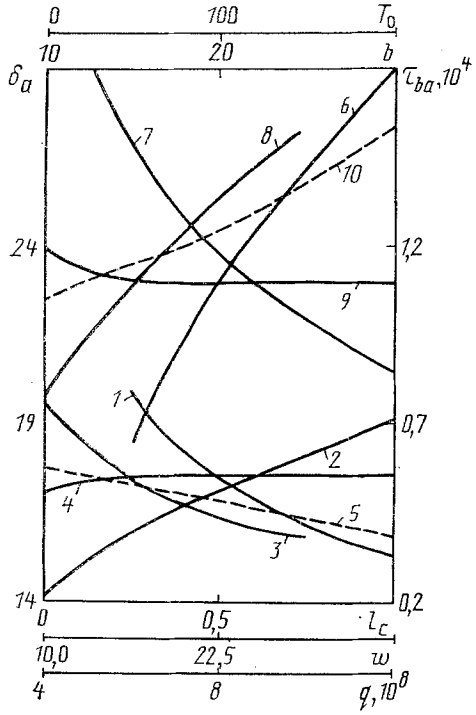

Fig. 6. Mean values of relative elongation δ_a (1-5) and time of complete elimination of intracrystallite liquation τ_{ba} (6-10) vs l_c (1, 6), w (2, 7), q (3, 8), b (4, 9), and T_0 (5, 10). δ_a, %; τ_{ba}, sec.

Using the formulas similar to [3], we have also determined mean values m_{0a}, S_{0a}, Q_a, ρ_{0a}, σ_{ba}, $\sigma_{0.2a}$, δ_a, and τ_{ba} of the parameters m_0, S_0, Q, ρ_0, σ_b, $\sigma_{0.2}$, δ, and τ_b, respectively.

The parameters m_{0a}, Q_a increase with increasing l_c, q, T_0 and decreasing w, b (Figs. 3, 4). The quantity S_{0a}, ρ_{0a} increases with increasing l_c, q, T_0 and decreasing w, b. All the above parameters practically do not change after b = 16 mm.

Mean values V_a, γ_a, n_a of the relative volume, radius and density of pores determined by formulas analogous to (3) are listed in Table 1. The parameter V_a decreases with increasing l_c, b, decreasing w and nonmonotonically depends on q, T_0, and attains its minimal values at $q = 6 \cdot 10^8$ W/m^2·K and $T_0 = 20$°C. The parameter γ_a increases with increasing b, decreasing T_0, and nonmonotonically changes in dependence on l_c, w, q. It has maximal values at $l_c = 0.5$ mm, w = 25 mm/sec, $q = 6 \cdot 10^8$ W/m^2·K. The quantity n_a decreases with q, b and behaves nonmonotonically with increasing l_c, w, T_0, attaining its minimal values at l_c = 0.5 mm, w = 25 mm/sec and maximal values at $T_0 = 20$°C.

Analysis has been also made of metal hardening in the case of laser hardening of the plate prepared from 08Kh18N10T steel when w = 30 mm/sec, a depth of melting through the metal being 3 mm. This value is between the predicted values x_b and x_m equal to 2.92 and 3.46 mm, respectively. According to [4], the sizes of crystalline grains in the steel crystallized after laser treatment involving flashing off the material are 3-20 μm. These values are determined by the ξ values which lie in the given range (7-14 μm).

CONCLUSIONS

1. A thickness of the dendritic axes of the first order and a distance between secondary branches of dendrites nonmonotonically change with respect to a thickness of the layer to be hardened. At first they decrease as the distance from the plate surface becomes longer, attain their maximal values, then decrease, and increase once more after attaining their maximum values.

2. Mean values of the above dendrite parameters increase with the temperature of the metal before laser treatment, density, and width of the zone of laser radiation action. They increase as the treatment rate and plate thickness decrease.

3. The crystalline structure of the laser-hardened metal is more dense and fine-dispersed than in ingots and cast pieces.

4. The mean thickness and volume share of inclusions of excess components change with respect to the hardened layer cross section in the same manner as the parameters of a dendritic structure. A specific surface of these inclusions decreases at a distance from the upper surface of the plate, attains its minimal value, then decreases and after attaining its maximum again decreases.

5. Ultimate strength, yield stress, relative elongation and dislocation density nonmonotonically change with respect to a thickness of the hardened layer similarly to S_0. The time of complete elimination of intracrystallite liquation at homogenizing annealing also nonmonotonically changes in the same manner as ξ and η.

6. The dependences of pore formation on laser treatment characteristics are established. It is shown that the mean relative pore volume decreases with increasing l_c, b, decreasing w and nonmonotonically depends on q, T_0. A mean value of the pore radii increases with increasing b, decreasing T_0, and nonmonotonically changes with l_c, w, q. A mean value of a pore density decreases with increasing q, b and nonmonotonically changes with increasing l_c, w, T_0.

7. The calculation results are in fair agreement with experimental data. They may be used to predict the structure and properties of the hardened metal subjected to laser treatment with flashing out.

LITERATURE CITED

1. P. A. Leont'ev, M. G. Khan, and T. N. Chekanova, Laser Surface Treatment of Metals and Alloys [in Russian], Moscow (1986).
2. A. G. Grigor'yants, Fundamental Principles of Laser Treatment of Materials [in Russian], Moscow (1989).
3. V. S. Kovalenko, A. D. Verkhoturov, L. F. Golovko, and I. A. Podchernyaeva, Laser and Electroerosion Hardening of Materials [in Russian], Moscow (1986).
4. M. A. Krishtal, A. A. Zhukov, and A. N. Kokora, The Structure and Properties of Laser-Hardened Alloys [in Russian], Moscow (1973).
5. V. V. Sobolev and P. M. Trefilov, Inzh.-Fiz. Zh., **62**, No. 1, 36-40 (1992).
6. V. V. Sobolev and P. M. Trefilov, Izv. Akad. Nauk SSSR, Metally, No. 5, 53-60 (1988).
7. V. V. Sobolev and P. M. Trefilov, Stal', No. 1, 39-42 (1989).
8. M. Flemings, Hardening Processes [Russian translation], Moscow (1977).
9. R. Éllist, Control of Eutectic Hardening [in Russian], Moscow (1987).
10. V. S. Zolotarevskii, The Structure and Strength of Cast Aluminum Alloys [in Russian], Moscow (1981).
11. V. V. Sobolev and P. M. Trefilov, Thermophysics of Metal Hardening Under Continuous Casting Conditions [in Russian], Moscow (1988).
12. V. V. Sobolev and P. M. Trefilov, Heat and Mass Transfer Processes Involving Hardening of Continuously Cast Ingots [in Russian], Krasnoyarsk (1984).
13. V. T. Borisov, The Two-Phase Zone Theory of a Metal Ingot [in Russian], Moscow (1987).
14. A. N. Kuznetsov, V. V. Sobolev, M. P. Borgoyakov, et al., Dokl. Akad. Nauk SSSR, **314**, No. 6, 1404-1407 (1990).